

Heat transfer within a microstructured polymer optical fibre preform

Katja Lyytikäinen^{1,2}, Joseph Zagari^{1,3}, Geoff Barton³, John Canning¹

¹Australian Photonics Cooperative Research Centre, Optical Fibre Technology Centre, University of Sydney, 206 National Innovation Centre, Australian Technology Park, Eveleigh NSW 1430, Australia

k.lyytikainen@ofc.usyd.edu.au, j.canning@ofc.usyd.edu.au

²School of Physics, University of Sydney, Sydney, NSW 2006, Australia

³Department of Chemical Engineering, University of Sydney, Sydney, NSW 2006, Australia

j.zagari@ofc.usyd.edu.au, barton@chemeng.usyd.edu.au

Short title: Heat transfer within a microstructured polymer optical fibre preform

Classification numbers: 44, 02.60.-x, 81.05.Lg

Abstract: Preform heating is one of the most important steps in the polymer fibre fabrication process due to the potential distortion that can be introduced when exposing the structure to high temperatures. Such heating is further complicated when internal air-structures are introduced into the preform - such as in Microstructured Polymer Optical Fibre (MPOF) preforms. The aim of this study was thus to investigate heat transfer in an MPOF preform. The effect of air-structure was studied using both numerical heat transfer simulations and preform heating experiments. A two-dimensional conductive heat transfer model with surface radiation was used in simulating the transient heat transfer in MPOF preforms with the results compared to those for a solid preform. It was found that relatively long heating times were required to reach a uniform temperature distribution within a preform, and that depending on the preform's air fraction its centre could heat up either faster or slower than a solid preform. Experimental tests where both a solid and an air-structured preform were heated in a drawing furnace with internal temperatures measured across the preform, confirmed the findings from the numerical simulations.

1 Introduction

Photonic crystal fibres, also known as microstructured or 'holey' fibres, were first developed in 1974 [1]. During the past few years, considerable effort has been devoted to researching their fabrication, properties and applications [2-5]. Such fibres are usually made from a single material in which the light guidance is defined by the air-structure, consisting of a number of air capillaries running along the length of the fibre surrounding either a solid or an air core. By changing the air-structure a wide range of fibre properties - such as dispersion [6], birefringence [7] and nonlinearities [8] - can be tailored to the required application. Traditionally photonic crystal fibres have been manufactured from silica or other glasses. Due to advantages such as low manufacturing cost and increased material flexibility, polymer was soon recognized a potential material for photonic crystal fibres [9, 10]. A number of studies have since been conducted in the area [11-13] and a strong potential for the development of high bandwidth optical fibres for LAN applications has been identified.

In addition to the wide range of properties that can be realised with MPOF, the manufacturing process is greatly simplified compared to traditional polymer fibres where complicated polymerisation processes may be required. A range of different fabrication methods can be used to make MPOF preforms such as capillary stacking, extrusion, polymerisation in a mould, drilling, casting and injection moulding. The MPOF preforms used in this study were fabricated using commercially available polymethylmethacrylate (PMMA) rods. The air structure was created by drilling the hole pattern using a computerised mill. The fibre is fabricated in a similar manner to conventional polymer fibres. The preform is heated to 160-250°C in a furnace and drawn down to 0.15-1.5mm diameter fibre in a drawing tower. Figure 1 shows an optical micrograph of a single-mode MPOF with a cladding diameter of 260µm and hole diameters of 2µm .

In order to manufacture microstructured fibres with the required optical properties, it is essential to retain the designed air-structure from the preform stage. The presence of air holes within the polymer will affect the temperature of the preform during the heating process, as well as creating additional surface tension forces that can distort the structure. It is thus important to understand the effect of the air-structure on the heat transfer during the fibre fabrication process. There are numerous studies on the heat transfer occurring within the manufacture of conventional silica optical fibres [14-16]. Despite the recent interest in photonic crystal fibres, very few heat transfer studies have been published where the effect of air structures within silica optical fibres has been considered [17-20]. In addition, due to the very different material properties of PMMA from silica these studies do not directly apply to MPOF fabrication, while the furnace designs and fabrication techniques differ greatly between the two cases. Heat transfer in solid polymer preforms has been studied by Reeve *et al.* [21, 22]. These studies provide a detailed investigation of the polymer preform heating process, however they cast no light on the effects that internal preform structures have on the heat transfer.

In this paper, we present a preliminary study of the heat transfer in polymer optical fibre preforms with an internal air-structure. The effect of the air-structure is studied using both numerical heat transfer modelling and experimental measurements. The heat transfer is simulated across the preform using a two-dimensional, time-dependent model. Three air-structured preforms with different air-fractions and a solid preform are considered.

2 Model description

To simulate heat transfer in an MPOF preform, a commercial finite element program was used for both the solid and air-structured cases. The preform was assumed to be infinitely long and allowed for an arbitrary hole pattern to be included. The air-structure design chosen for this study was an hexagonal arrangement of holes with three rings surrounding a solid core, as shown in Figure 2. An

axisymmetric two-dimensional model was also used to study the impact of ‘end effects’ on the temperature due to the finite length of the preforms used.

2.1 Model geometry

Figure 2a-c show the geometries used. In all cases examined, an infinite cylinder of polymer was assumed with an outer diameter of 50 mm and 72 air holes positioned in a hexagonal pattern. The geometries differ in that the air fraction of the air-structured section is 0.4 for Preform A, 0.7 for Preform B and 0.1 for Preform C. These differences were achieved by keeping the hole positions the same but varying the hole diameter from 2.0 mm (A) to 2.6 mm (B) to 1.0mm (C). Note that for comparative purposes, a ‘solid case’ was also simulated by assigning polymer properties to the holes without changing either the hole geometry or the finite element meshing.

The two-dimensional axisymmetric case was used to take into account the finite length of the preform when it became clear that heat transfer from the ends was having a major impact on the internal temperature profile. Figure 3 shows the geometry employed, consisting of a ‘layered cylinder’ of finite length. The model (assuming circular symmetry in the radial direction) consisted of two layers of polymer with one layer of air in between. The air hole pattern in this case was approximated by one circular layer of air, with the diameter of the preform again being 50 mm while the air layer thickness was 5 mm.

2.2 Heat transfer model and numerical solution

Heat transfer within the preform was assumed to occur by conduction only for which the time dependent conduction equation is expressed in Equation (1),

$$\mathbf{r}c_p \frac{\partial T}{\partial t} = \nabla \cdot (k\nabla T) \quad (1)$$

where \mathbf{r} is density, c_p is specific heat capacity, T is temperature, t is time and k is the thermal conductivity. The boundary condition at the surface of the preform is given by Equation (2). A constant heat transfer coefficient, h , was used while the external temperature, T_{ext} , was set to the measured furnace air temperature, 130°C. The initial temperature within the entire polymer rod was set to 24°C, that is at the ambient value external to the furnace. Radiative heat transfer from the external surface was taken into account via a constant surface emissivity, ϵ . Note that \mathbf{s} is the Stefan-Boltzmann constant. The contribution of ‘internal’ radiative heat transfer within the polymer rod was neglected.

$$-k \frac{\partial T}{\partial n} = h(T - T_{ext}) + \mathbf{se}(T^4 - T_{ext}^4) \quad (2)$$

The polymer properties were taken as those of PMMA and the gas properties as those of air. The physical properties for both are listed in Table 1. The thermal conductivity for PMMA was adjusted to fit the experimental results, as no measured data were available for the specific grade of PMMA material used in this study. This adjusted value is of the same order of magnitude as that reported in the literature (0.19 W/mK) for other grades of PMMA [23]. An estimated (from engineering correlations) value of 8 W/mK was used for the external heat transfer coefficient, h .

Table 1: Material properties

Material	PMMA	Air
Density ρ [kg/m ³] [23]	1170	0.93
Specific heat capacity C_p [J/kgK] [23]	1380	1010
Thermal conductivity k [W/mK]	0.15	0.032
Emissivity ϵ [21]	0.96	-

A computational software package [24] was used to solve the heat conduction equation which was discretized using a finite element method. The matrix equations resulting from the discretisation were solved with a band matrix solver from LAPACK based on an LU decomposition. Variable time step sizes were used - from 0.5s at the beginning where the temperature changes were the greatest, to 400s as the preform moved towards thermal equilibrium, totalling some 130 steps for a heating period of five hours. Due to the complex air hole structure, a non-uniform grid was employed. As an example, the mesh for Preform A is shown in Figure 4 consisting of an unstructured mesh of 6700 bilinear elements. For the axisymmetric model, a uniform structured mesh with quadrilateral elements was used consisting of 1000 elements. A typical simulation for the axisymmetric model was 55 CPU seconds on a single processor SGI Origin 2000 computer. For the two-dimensional infinite length model case (with its larger number of elements), 300 CPU seconds were required on the same computer.

For this study, the numerical results were compared with those for an analytical solution for an infinite cylinder with a homogeneous cross-sectional structure. The results agreed well provided small enough time steps were used. The effects of alternative meshing were also tested by simulating a two-dimensional infinite cylinder with one air-layer using both unstructured and structured meshes. The results were found to be identical for both cases.

3 Heat transfer experiments

In order to validate the heat transfer modelling work, experiments were conducted with MPOF preforms. These preforms were prepared from 5cm diameter extruded PMMA with a length of 140mm. Both a solid and an air-structured preform were used. The air-structure was the same as that for Preform A shown in Figure 2a with 2mm holes extending throughout the entire length.

A convection type furnace was used in these experiments, with the preform suspended in a metal cylinder hung within the furnace chamber and hot air blown in via a ring of holes situated near the centre of the metal cylinder (Figure 5a). T-type thermocouples were embedded in the preform to measure the temperature at various positions during the heating-up process, see Figure 5b. The thermocouple holes extended down some 70mm to the position of the 'hot-zone' created by the hot air inlets. The airflow through the holes was restricted by blocking them at both ends of the preform. The heating was very efficient in that the furnace air temperature reached its set value in two minutes from room temperature. A temperature lower than the usual PMMA draw temperature was used so that the preform did not deform while being heated. The oven temperature was set at 130°C while the preform was heated up over a period of two hours.

Figure 6 shows a comparison between simulated and measured data for air-structured Preform A at a position 2mm from the preform surface and in the centre of the rod. In the initial modelling work radiative heat transfer from the surface was ignored, however it soon became apparent that this mode of heat transfer could not be omitted. After inclusion of the thermal radiation term, the simulated temperatures showed good agreement with the measured values. Again it must be noted that the thermal conductivity of the polymer was adjusted such that the simulated data (after radiative heat transfer was included) matched the experimental data as closely as possible. No other parameters were adjusted.

The measured temperatures steadied out to a lower temperature than the oven air temperature, as can be seen from Figure 6. This was felt to be due to the finite length of the preform, which was not taken into account in the simulations that assumed an infinitely long cylinder. Figure 7 shows temperature contour plots at 2, 3 and 4hr from the axisymmetric model, where the finite length of the preform was taken into account. As can be seen from Figure 7 there is hardly any change between 3 and 4hr of heating while the top half of the preform has steadied out to a lower temperature than the furnace temperature of 130°C. These simulation results showed that the measured lower steady-state temperature was almost certainly due to heat loss from the preform top end which was exposed to a lower air temperature. The initial heating-up phase (that is, well before the temperatures began to

approach their equilibrium values), however, agreed well with the two-dimensional infinite cylinder model, which could thus be used to study the effect of air structures on heat transfer in MPOF's.

4 Results and Discussion

Simulations were conducted for four different geometries to study the effect of air structure - a solid rod and three air-structured preforms, Figure 2, having different air fractions. Preform A, B and C had air fractions of 0.4, 0.7 and 0.1, respectively, where the air fraction is defined as the area of the holes relative to the total hexagonal structured area. A temperature contour plot for Preform A after 30 minutes of heating is shown in Figure 8. The contours in the air-structured region show the effect of the holes on the temperature profile.

The radial temperature profiles as a function of time are plotted in Figure 9 for both the solid cylinder case and for Preform A. Significant differences between the solid and structured cases are evident after five minutes of heating. The temperature in the outer part of the preform rises, relative to the solid case, as the air holes act as a resistive heat barrier. Note however that the entire structured preform heats up faster than the solid case. Such behaviour was unexpected, as it was initially felt that the presence of the air holes would slow down heat transfer into the central region of the preform. The results indicate that the relatively low thermal capacity of the air (which meant that the heat transfer across the holes was always essentially at pseudo steady-state) together with the fact that the structured preform contains less polymer than the solid case, resulted in a faster dynamic response in the central portion of the structured preform than expected.

Figure 10 shows the corresponding experimental results from comparing the heating of the solid rod and the structured Preform A. The measured temperatures, see Figure 5b, are plotted according to their distance from the centre at various times from the start of the heating process. This experimental data confirms the findings from the simulations in that the structured preform heats up faster than the solid preform.

Figure 11 shows the simulated heating-up phases for the three structured preforms and the solid case. After only five minutes differences between the preforms start to be seen. The outer part of the preform heats up faster for all the structured preforms when compared to the solid case, such that a higher air fraction results in faster heating. The centre of the preform heats up faster than the solid case for all the structured preforms except for Preform C which had the lowest air fraction. After 20 minutes heating, the centre of Preform C is 1°C lower than the solid case. This result indicates that there exists an air fraction below which the impact of greater thermal resistance of the air structure exceeds the impact of lower thermal mass and results in slower heating of the preform centre.

Both the solid and the structured preforms reached the furnace temperature after some 2.5hr of heating. This is a relatively long time in production terms and illustrates the basic problem with this type of heating where the outer part of the preform will reach the fibre draw temperature before the central part. This situation can result in deformation of the structure with the hotter outer part drawing at a different rate to the cooler inner part. Such behaviour has certainly been observed in our drawing experiments, this fact being one of the prime reasons for the current study on preform heating. In order to minimise such potential problems, alternative heating schemes can be employed to provide uniform, symmetric heating. Other types of heating methods such as infrared or microwave heating may be advantageous.

5 Conclusions

Heat transfer within an air-structured PMMA optical fibre preform was numerically simulated where it was found that despite the relatively low temperatures, it was necessary to include radiative heat transfer in the model. The heat transfer model was validated against experimental data. Heat transfer between air-structured and solid preforms was also compared. It was found that depending on the air fraction of the structured preform its centre could heat up either faster or slower than the centre of a solid preform. At higher air fractions (here 0.4 and 0.7), the structured preform heated up faster than the solid preform due to the effect of reduced thermal mass being greater than the effect of the thermal resistance of the air holes. At a lower air fraction (here 0.1), the centre of the preform heated up slower than the solid preform centre.

The hexagonal hole pattern used distorted the temperature profile only slightly from a radially symmetric case. This distortion was greater for the higher air fraction, indicating that preforms with highly asymmetric hole structures and a high air fraction could experience radially asymmetric temperature profiles. In order to produce structured optical fibres with undistorted structures, the heating process must be optimised so that any asymmetries are minimised. The heat transfer model used in this study enables simulations with arbitrary hole structures to be examined, and thus can be used both in optimising the preform heating conditions and also as a tool in designing the heating furnace. Tighter characterisation of the properties of the specific PMMA grades used would further improve the quantitative results, although in this case only a modest adjustment was required to achieve an acceptably close fit between simulated and experimental temperature profiles.

6 Acknowledgements

The authors would like to acknowledge the help of the following people who have contributed to this study: Barry Reed, Geoff Henry, Alex Argyros, Steven Manos, Martijn van Eijkelenborg, Maryanne

Large, Pam McNamara, Simon Fleming, Simin Nasser and Roger Tanner. They would also like to acknowledge CSC - Scientific Computing for use of their software and computing resources.

7 References

- [1] P. Kaiser and H. W. Astle, "Low-loss single-material fibers made from pure fused silica," *The Bell System Technical Journal*, vol. 53, pp. 1021-1039, 1974.
- [2] P. Russell, "Photonic crystal fibers," *Science*, vol. 299, pp. 358-62, 2003.
- [3] J. Knight, J. Broeng, T. Birks, and P. Russell, "Photonic band gap guidance in optical fibers," *Science*, vol. 282, 1998.
- [4] J. Knight, T. Birks, and P. Russell, "'Holey' silica fibers, Chapter 2," in *Optics of Nanostructured Materials*, V. A. Markel and T. F. George, Eds. New York: Wiley, 2001, pp. 39-71.
- [5] T. M. Monro, D. J. Richardson, N. G. Broderick, and P. J. Bennett, "Holey optical fibres: an efficient modal model," *Journal of Lightwave Technology*, vol. 17, pp. 1093-1102, 1999.
- [6] A. Ferrando, E. Silvestre, and P. Andres, "Designing the properties of dispersion-flattened photonic crystal fibers," *Optics Express*, vol. 9, pp. 687-697, 2001.
- [7] A. Ortigosa-Blanch, J. C. Knight, W. J. Wadsworth, J. Arriaga, B. J. Mangan, T. A. Birks, and P. S. J. Russell, "Highly birefringent photonic crystal fibers," *Optics Letters*, vol. 25, pp. 1325-27, 2000.
- [8] P. Petropoulos, T. M. Monro, W. Belardi, K. Furusawa, J. H. Lee, and D. J. Richardson, "2R-regenerative all-optical switch based on a highly nonlinear holey fiber," *Optics Letters*, vol. 26, pp. 1233-35, 2001.
- [9] M. A. v. Eijkelenborg, M. C. J. Large, A. Argyros, J. Zagari, S. Manos, N. A. Issa, I. M. Bassett, S. Fleming, R. C. McPhedran, C. M. d. Sterke, and N. A. P. Nicorovici, "Microstructured polymer optical fibre," *Optics Express*, vol. 9, pp. 319-327, 2001.
- [10] H. Han, H. Park, M. Cho, and J. Kim, "Terahertz pulse propagation in plastic photonic crystal fibres," presented at The 4th Pacific Rim Conference on Lasers and Electro-Optics, Chiba, Japan, post-deadline paper, 2001.
- [11] M. C. J. Large, M. A. v. Eijkelenborg, A. Argyros, J. Zagari, S. Manos, N. A. Issa, I. M. Bassett, S. Fleming, R. C. McPhedran, C. M. d. Sterke, and N. A. P. Nicorovici, "Microstructured polymer optical fibres: a new approach to POFs," presented at Plastic Optical Fibres Conference, Amsterdam, The Netherlands, 2001.
- [12] J. Choi, D. Kim, and J. Paek, "Fabrication and properties of polymer photonic crystal fibres," presented at Plastic Optical Fibres Conference, Amsterdam, The Netherlands, 2001.
- [13] M. A. v. Eijkelenborg, A. Argyros, G. Barton, I. M. Bassett, M. Fellow, G. Henry, N. A. Issa, M. C. J. Large, S. Manos, W. Padden, L. Poladian, and J. Zagari, "Recent progress in

- microstructured polymer optical fibre fabrication and characterization," *Optical Fiber Technology*, vol. 9, accepted 16.6.2003, 2003.
- [14] S. R. Choudhury and Y. Jaluria, "A computational method for generating the free-surface neck-down profile for glass flow in optical fiber drawing," *Numerical Heat Transfer, Part A*, vol. 35, pp. 1-24, 1999.
- [15] S. R. Choudhury and Y. Jaluria, "Thermal transport due to material and gas flow in a furnace for drawing an optical fiber," *Journal of Material Research*, vol. 13, pp. 494-503, 1998.
- [16] G. K. Gupta, W. W. Schultz, E. M. Arruda, and X. Lu, "Nonisothermal model of glass drawing stability," *Rheologica Acta*, vol. 35, pp. 584-596, 1996.
- [17] A. D. Fitt, K. Furusawa, T. M. Monro, and C. P. Please, "The mathematical modelling of capillary drawing for holey fibre manufacture," *Journal of Engineering mathematics*, vol. 43, pp. 201-27, 2002.
- [18] K. Lyytikäinen, P. Råback, and J. Ruokolainen, "Numerical simulation of a specialty optical fibre drawing process," presented at 4th International ASME/JSME/KSME Symposium on Computational Technology (CFD) for Fluid/ Thermal/ Chemical/ Stress Systems and Industrial Applications, Vancouver, BC, Canada, 2002.
- [19] G. Deflandre, "Modeling the manufacturing of complex optical fibers: the case of the holey fibers," presented at 2nd International Colloquium of Modelling of Glass Forming and Tempering, Valenciennes, France, 2002.
- [20] P. Gospodinov and A. L. Yarin, "Draw resonance of optical microcapillaries in non-isothermal drawing," *International Journal of Multiphase Flow*, vol. 23, pp. 967-76, 1997.
- [21] H. M. Reeve, A. M. Mescher, and A. F. Emery, "Experimental and numerical investigation of polymer preform heating," *Journal of Materials Processing & Manufacturing Science*, vol. 9, pp. 285-301, 2001.
- [22] H. M. Reeve, A. M. Mescher, and A. F. Emery, "The effect of natural convection heating instabilities on the diameter of polymer optical fiber," presented at 11th International Plastic Optical Fibres Conference 2002, Tokyo, Japan, 2002.
- [23] D. W. v. Krevelen, *Properties of polymers, their estimation and correlation with chemical structure*, 2nd ed. Amsterdam, New York: Elsevier Scientific Pub. Co., 1976.
- [24] CSC - Scientific Computing Ltd, "ELMER, Computational resource in research and development," <<http://www.csc.fi/elmer/>>, 21.1.2003.

Table of Figures

Figure 1. Optical micrographs of a single-mode MPOF with hole diameters of $2\mu\text{m}$ and spacing of $5\mu\text{m}$

Figure 2. Schematics representations of the model geometry for the two-dimensional infinite cylinder case with air-structured air fractions of (a) 0.4, (b) 0.7, and (c) 0.1.

Figure 3. Schematics of the geometry for the axisymmetric case (a) preform cross-section (b) model geometry

Figure 4. (a) Unstructured mesh used for Preform A. The mesh used for the air holes is shown as an inset. (b) Structured mesh used for the axisymmetric model.

Figure 5. (a) Heating experiment set-up, preform inside the furnace. (b) Cross-section of the preform showing thermocouple positions (filled circles).

Figure 6. Measured vs. simulated data for an air-structured preform

Figure 7. Temperature contour plot of the axisymmetric model after 2, 3 and 4 hr of heating

Figure 8. Temperature contour plot for Preform A at time 30min, contour lines every 5°C

Figure 9. Radial temperature profiles across the preform at different heating times, comparison of the solid rod and Preform A. Vertical lines show the position of the air-hole structure within the preform.

Figure 10. Experimental heating results. Radial temperature profiles across the preform at different heating times: comparison of the solid rod and Preform A.

Figure 11. Radial temperature profiles at different heating times, comparison of the air-structured Preforms A, B, and C with air fractions 0.4, 0.7, and 0.1, respectively.

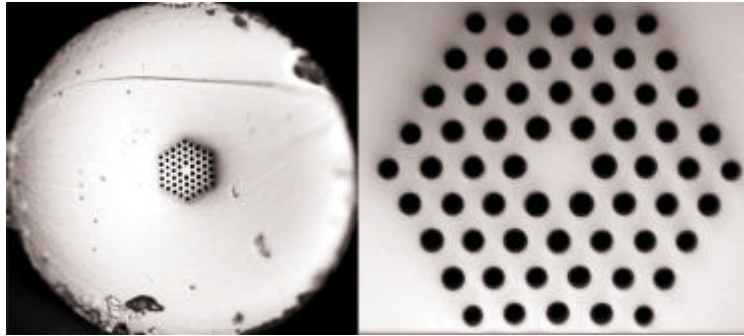


Figure 1. Optical micrographs of a single-mode MPOF with hole diameters of $2\mu\text{m}$ and spacing of $5\mu\text{m}$

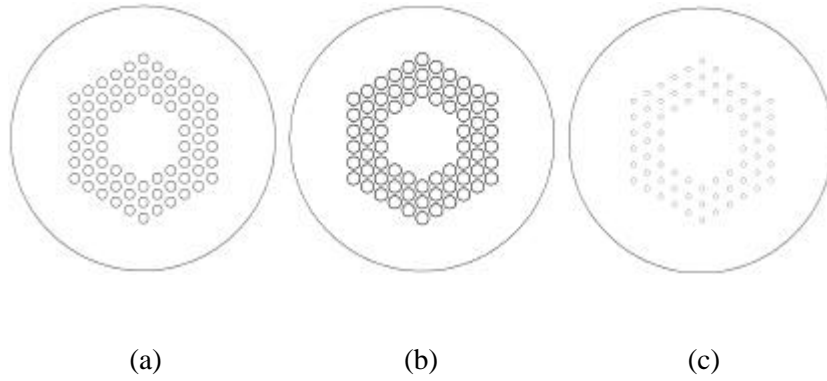


Figure 2. Schematics representations of the model geometry for the two-dimensional infinite cylinder case with air-structured air fractions of (a) 0.4, (b) 0.7, and (c) 0.1.

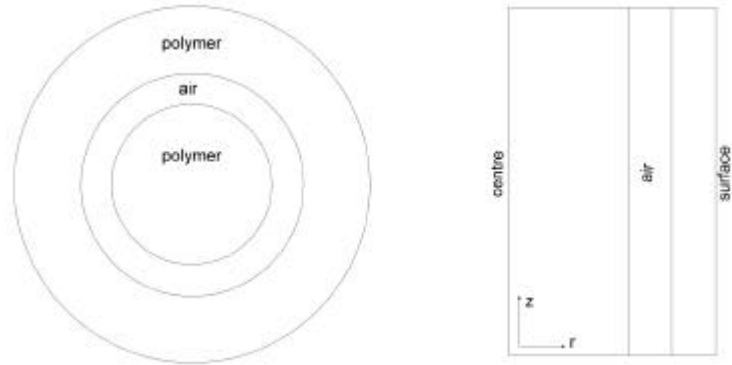
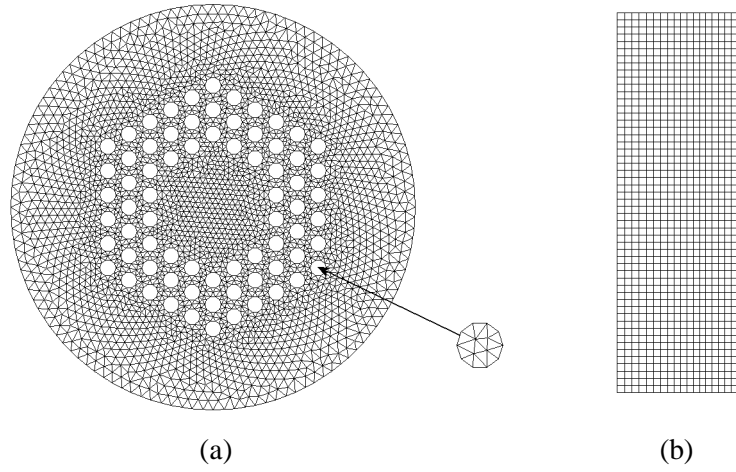


Figure 3. Schematics of the geometry for the axisymmetric case (a) preform cross-section (b) model geometry



**Figure 4. (a) Unstructured mesh used for Preform A. The mesh used for the air holes is shown as an inset.
(b) Structured mesh used for the axisymmetric model.**

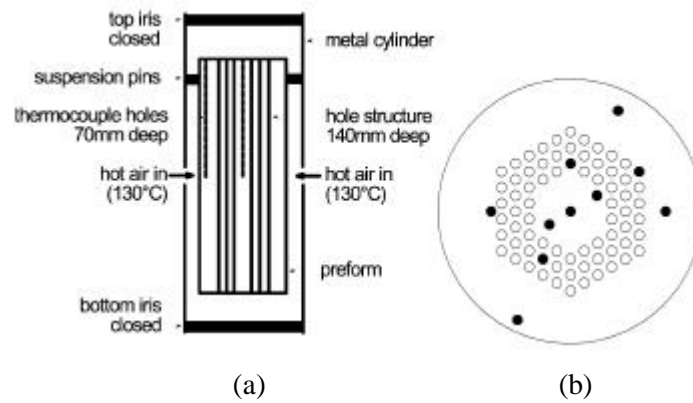


Figure 5. (a) Heating experiment set-up, preform inside the furnace. (b) Cross-section of the preform showing thermocouple positions (filled circles).

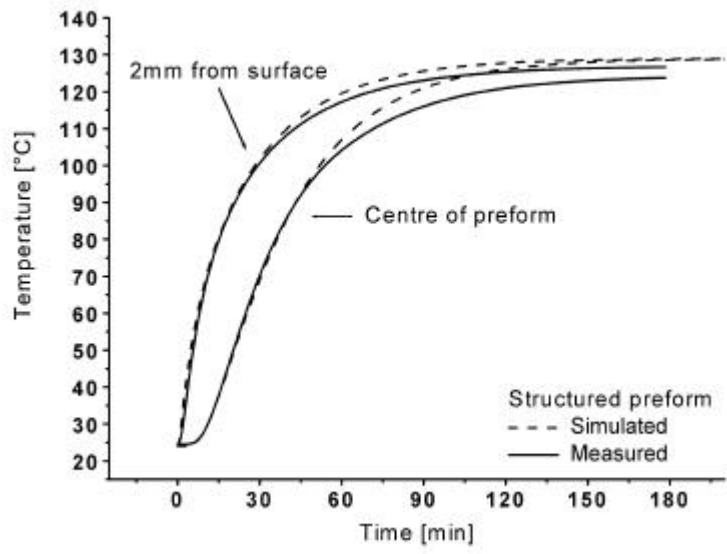


Figure 6. Measured vs. simulated data for an air-structured preform

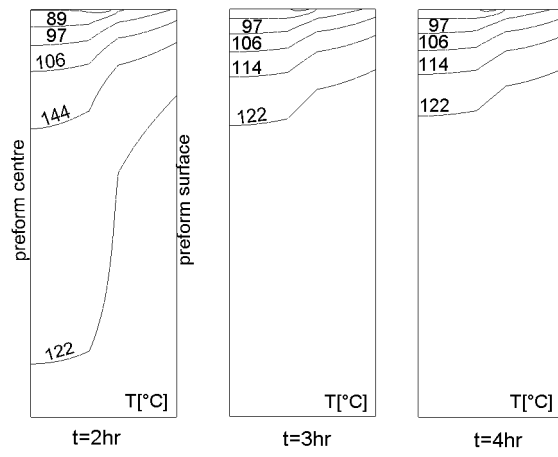


Figure 7. Temperature contour plot of the axisymmetric model after 2, 3 and 4 hr of heating

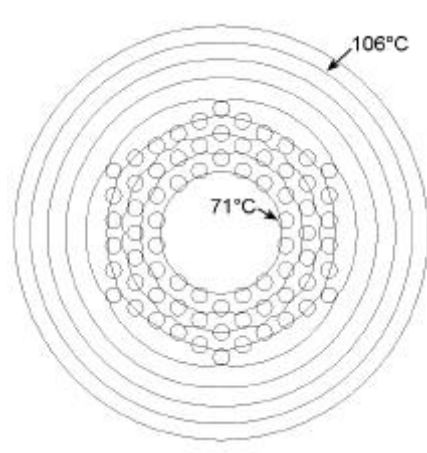


Figure 8. Temperature contour plot for Preform A at time 30min, contour lines every 5°C

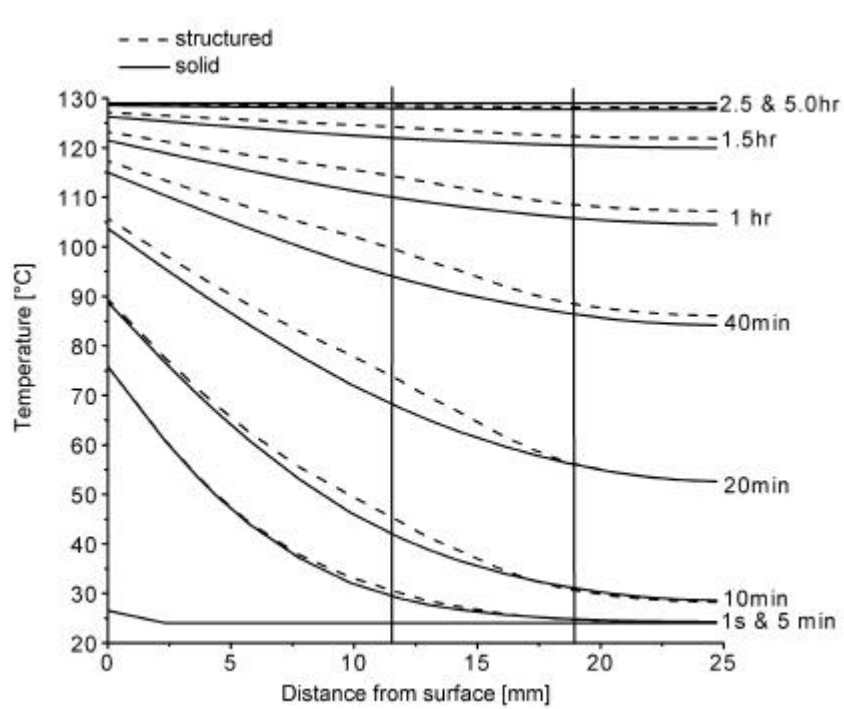


Figure 9. Radial temperature profiles across the preform at different heating times, comparison of the solid rod and Preform A. Vertical lines show the position of the air-hole structure within the preform.

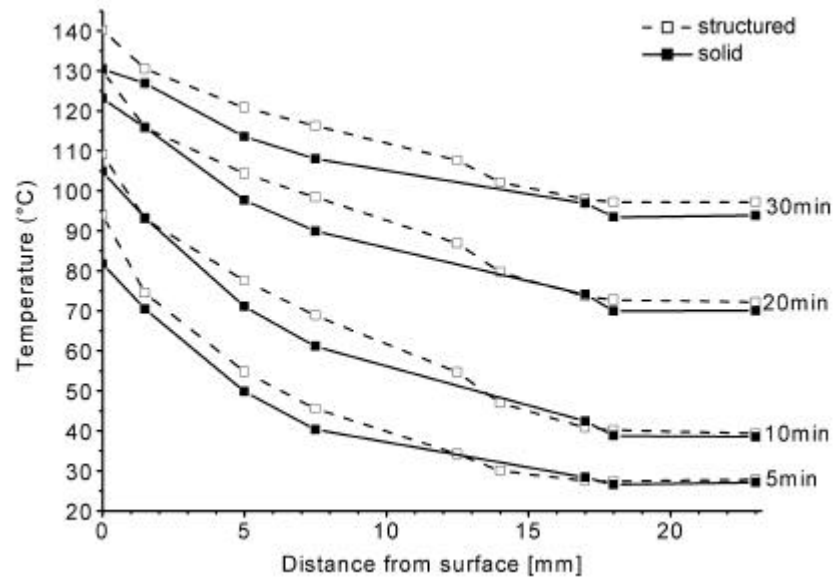


Figure 10. Experimental heating results. Radial temperature profiles across the preform at different heating times: comparison of the solid rod and Preform A.

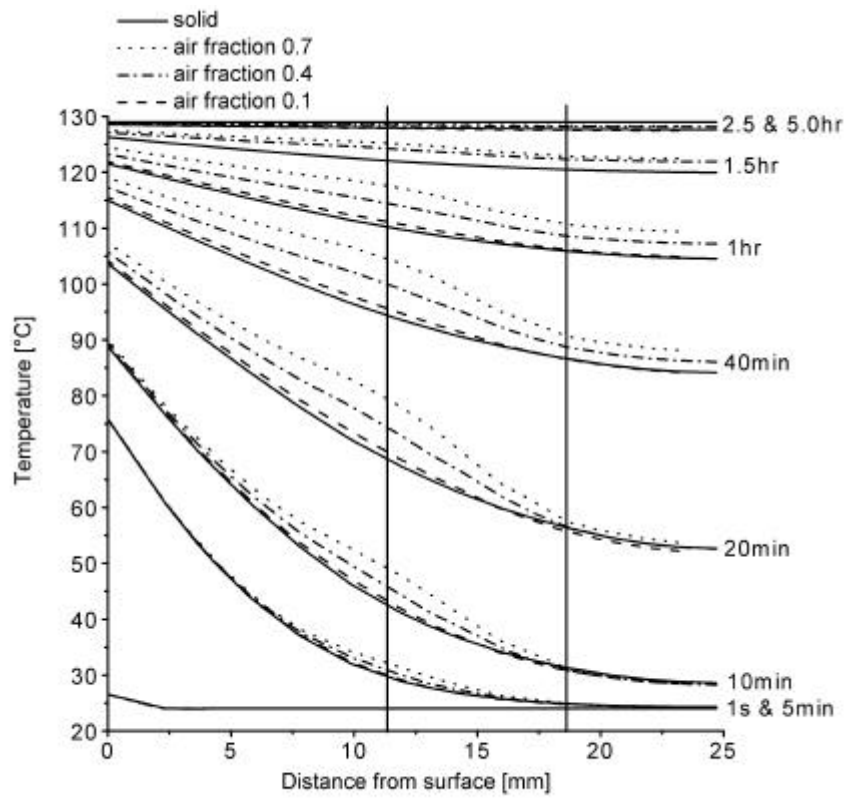


Figure 11. Radial temperature profiles at different heating times, comparison of the air-structured Preforms A, B, and C with air fractions 0.4, 0.7, and 0.1, respectively.